PROCEEDINGS OF SCIENCE

The NRQCD Υ spectrum at non-zero temperature using Backus-Gilbert regularisations

Antonio Smecca,[a,*] **Gert Aarts,**[a] **Chris Allton,**[a] **Ryan Bignell,**[a,b] **Timothy J. Burns,**[a] **Benjamin Jäger,**[c] **Rachel Horohan D'Arcy,**[d] **Seyong Kim,**[e] **Maria-Paola Lombardo,**[f] **Ben Page,**[a] **Sinéad M. Ryan,**[b] **Tom Spriggs**[a] **and Jon-Ivar Skullerud**[b,d]

[a] *Department of Physics, Swansea University, Swansea, SA2 8PP, United Kingdom*
[b] *School of Mathematics, Trinity College, Dublin, Ireland*
[c] *Quantum Field Theory Center & Danish IAS, Department of Mathematics and Computer Science , University of Southern Denmark, 5230, Odense M, Denmark*
[d] *Department of Physics and Hamilton Institute, National University of Ireland Maynooth, County Kildare, Ireland*
[e] *Department of Physics, Sejong University, Seoul 143-747, Korea*
[f] *INFN, Sezione di Firenze, 50019 Sesto Fiorentino (FI), Italy*

E-mail: antonio.smecca@swansea.ac.uk

Understanding how the properties of heavy mesons change as temperature increases is crucial for gaining valuable insights into the quark-gluon plasma. Information about meson masses and decay widths is encoded in the meson spectral function, which, in principle, can be extracted from Euclidean correlation functions via generalised Laplace transformations. However, this inverse problem is ill-posed for lattice correlation functions and requires regularisation. In this work, we present the latest results for bottomonium spectral functions obtained within the lattice NRQCD framework using the Backus-Gilbert regularisation, along with two other variants, one of which is commonly referred to as the HLT method. Our analysis employs Generation 2L anisotropic lattice configurations produced by the FASTSUM collaboration.

The 41st International Symposium on Lattice Field Theory (LATTICE2024)
28 July - 3 August 2024
Liverpool, UK

*Speaker

PoS(LATTICE2024)197

1. Introduction

Understanding the properties of heavy mesons at high temperatures is very important to gain insights on the QCD phase diagram. In particular, the dissociation of heavy quarkonia in a deconfined medium may serve as a thermometer for relativistic heavy-ion collisions [1, 2]. The abundant production of bottomonium systems in LHC heavy-ion collision experiments make them good probes of the quark-gluon plasma (QGP). Results from the CMS Collaboration indicate sequential suppression in this system [3].

For more than a decade, the FASTSUM collaboration has extensively studied bottomonium systems using lattice QCD simulations with anisotropic lattices and Wilson fermions [4–7]. Of particular interest in this investigation is the spectral function $\rho(\omega)$, which encodes information about meson masses and decay widths. This function can be extracted from Euclidean correlation functions through an inverse Laplace transform. However, the inverse problem is ill-posed when using lattice correlation functions, and several different methods have been developed over the years to overcome this obstacle.

This work builds on previous studies [8–12] of the bottomonium spectral functions using linear approaches to the inverse problem based on the Tikhonov and Backus-Gilbert methods [13–15]. For other studies of bottomonium spectral functions by the FASTSUM collaboration with non-linear methods see Refs. [16, 17].

2. Lattice ensembles

For this investigation, we used the Generation 2L gauge ensembles generated by the FASTSUM collaboration. The Wilson-clover fermion action was employed, with tree-level tadpole improvement with stout links, same parameters as the HadSpec collaboration [18], approximately 1000 configurations for each temperature, $m_\pi = 239(1)$ MeV, anisotropic lattices with anisotropy $\xi = 3.453(6)$ and $T_c = 167(2)$ MeV. In this work, we use the (earlier) scale setting from Ref. [19]. As such, the spatial lattice spacing is $a_s = 0.1136(6)$ fm. The strange quark has been tuned to its physical value via the tuning of the light and strange pseudoscalar masses [20, 21]. The estimate for $T_{\rm pc}$ comes from an analysis of the renormalised chiral condensate, which uses the updated lattice spacing of Ref. [22], that was implemented in our analysis in Ref. [23].

The bottom quarks are simulated using the non-relativistic QCD (NRQCD) effective theory [24] with power counting in the heavy quark velocity in the bottomonium rest frame, $v \sim |\boldsymbol{p}|/m_b$. In the NRQCD formalism only energy differences are physically significant, such that we can define the additive mass renormalisation from the following mass difference, finding

$$E_0 = M_{\rm exp}(\Upsilon) - M(\Upsilon) = 7463 \text{ MeV}, \tag{1}$$

where the lattice value of $M(\Upsilon)$ was determined using a single exponential fit to the zero-temperature correlator in the vector channel.

3. NRQCD spectral functions

To study the spectrum of bottomonium at high temperatures the best way forward is to employ methods that do not make any assumption on the spectral structure. For this reason, the observable

N_τ	128	64	56	48	40	36	32	28	24	20	16	12
T(MeV)	47	95	109	127	152	169	190	217	253	304	380	507

Table 1: FASTSUM Generation 2L ensembles used in this work. The lattice size is $32^3 \times N_\tau$, with temperature $T = 1/(a_\tau N_\tau)$. The temporal and spatial lattice spacing are respectively 0.03246(7) and $a_s = 0.11208(31)$ fm giving a renormalised anisotropy $\xi = a_s/a_\tau = 3.453(6)$ and the pion mass is $m_\pi = 239(1)$ MeV [25]. The estimate for $T_{\rm pc}$ comes from an analysis of the renormalised chiral condensate and equals $T_{\rm pc} = 167(2)(1)$ MeV [22, 23]. Full details of these ensembles may be found in Refs. [22, 23, 26].

of interest here is the spectral function $\rho(\omega)$. Extracting $\rho(\omega)$ from lattice correlators is an ill-posed problem that has recently attracted a lot of attention within the lattice community, as evidenced by three plenary presentations on the topic [27–29]. The access to $\rho(\omega)$ unlocked several important investigations using lattice simulations, such as the R-ratio for $e^+e^- \to$ hadrons [30], inclusive hadronic decays of the τ lepton [31, 32] and inclusive semi-leptonic decays of heavy mesons [33–38]. Other applications include neutrino-nucleon scattering [39–41] and advances in hadron spectroscopy [42–44]. For a study of the inverse problem in the continuum limit see Ref. [45].

In the relativistic formulation of lattice QCD, one can relate the Euclidean correlator to the spectral function through the following integral equation

$$G(\tau) = \int_0^\infty \frac{d\omega}{2\pi}\, \rho(\omega)\, K(\omega, \tau, T), \tag{2}$$

where $G(\tau)$ is the meson correlation function, and $K(\omega, \tau, T)$ is an integration kernel that depends on the temperature of the system.

In the NRQCD formalism one can re-write equation 2 as

$$G(\tau) = \int_{\omega_{\rm min}}^{\omega_{\rm max}} d\omega\, \rho(\omega)\, e^{-\omega\tau}, \tag{3}$$

where $\omega_{\rm max}$ is the energy cutoff and $\omega_{\rm min}$ is the minimum energy chosen to perform the integration [4, 5, 46].

Due to the finite volume of lattice simulations, the spectral density contained in LQCD correlators is a distribution that in order to be physically relevant needs to be convoluted with a *smeared* kernel. Smearing is needed to turn the distribution of δ-functions into a smooth function that can be studied in the infinite-volume limit [47]. Assuming an infinite number of time-slices τ, the Stone-Weierstrass theorem admits an exact polynomial expression for these smearing kernels

$$\overline{\Delta}(\omega, \omega_n) = \sum_{\tau=1}^{\infty} g_\tau(\omega_n) e^{-\omega\tau} \approx \delta(\omega - \omega_n), \tag{4}$$

which gives the exact model independent solution

$$\rho(\omega_n) = \int_{\omega_{\rm min}}^{\infty} d\omega\, \delta(\omega - \omega_n)\rho(\omega). \tag{5}$$

This is the central idea behind any linear method for spectral reconstruction.

Imagining to be in an *ideal* scenario where we have access to the exact correlator at infinite discrete times, one can obtain the spectral function following

$$\rho(\omega_n) = \int_{\omega_{\min}}^{\infty} d\omega\, \overline{\Delta}(\omega, \omega_n)\rho(\omega) = \int_{\omega_{\min}}^{\infty} d\omega \sum_{\tau=1}^{\infty} g_\tau(\omega_n) e^{-\omega\tau}\rho(\omega) = \sum_{\tau=1}^{\infty} g_\tau(\omega_n) G(\tau), \quad (6)$$

where in the last step we used the definition for $G(\tau)$ in equation 3.

3.1 Backus-Gilbert and Tikhonov methods

In realistic lattice QCD simulations, meson correlation functions are truncated by the maximum time extent of the lattice and are affected by statistical noise. This means that equation 4 can only be approximated with the given data. The consequence of this is that we can at most get an estimate for the spectral function as

$$\hat{\rho}(\omega_n) = \sum_{\tau=1}^{\tau_{\max}} g_\tau(\omega_n) G(\tau), \quad (7)$$

where $\tau_{\max}$ is the maximum time extent of the lattice and $\hat{\rho}(\omega_n)$ represents the estimate of $\rho(\omega)$ at ω_n.

The essential ingredient for the reconstruction of the spectral function is the calculation of the coefficients $g_\tau(\omega_n)$. Following standard methods like the Backus-Gilbert [13, 14] or Tikhonov [15], they are obtained minimising the functional

$$A^{\mathrm{BG,Tikh}}[\boldsymbol{g}] = \int_{\omega_{\min}}^{\omega_{\max}} d\omega\, [\overline{\Delta}^{\mathrm{BG,Tikh}}(\omega, \boldsymbol{g}) - \delta(\omega - \omega_n)]^2, \quad (8)$$

which can be understood as finding the smearing kernel closest to a δ-function. In the equation above, $\boldsymbol{g}$ corresponds to a vector of coefficients at different τ for a given ω. Our results were obtained setting $a_\tau\omega_{\min} = -0.1$ and $a_\tau\omega_{\max} = 1.0$. To preserve the scale of the spectrum, the chosen representation for the width functional is typically minimised in conjunction with a unit area constraint. In this case, the kernel approximation uses Legendre polynomials. There is an interesting alternative method based on Chebyshev polynomials [48] which we will not be discussed here.

The fact that we are facing an ill-posed (or rather ill-conditioned) problem is that the excessive minimisation of $A[\boldsymbol{g}]$ leads to gigantic coefficients, which once applied to the meson correlator lead to huge statistical errors, making the result useless from a physical point of view. An example of this can be seen in Figure 2 of Ref. [49]. To prevent the coefficients g_τ from reaching such large values, one needs to introduce an error functional $B[\boldsymbol{g}]$ and minimise the linear combination

$$W[\boldsymbol{g}] = \frac{A[\boldsymbol{g}]}{A[\boldsymbol{0}]} + \lambda B[\boldsymbol{g}], \quad (9)$$

where the error functional is defined as

$$B^{\mathrm{BG}}[\boldsymbol{g}] = \frac{\mathrm{Cov}_{\tau,\tau'}[\boldsymbol{g}]}{G(\tau=0)^2}, \qquad B^{\mathrm{Tikh}}[\boldsymbol{g}] = \mathbb{I}, \quad (10)$$

for the Backus-Gilbert and Tikhonov methods respectively, where Cov is the covariance matrix of the correlator and $\mathbb{I}$ is the identity matrix. The hyper-parameter λ determines how much the minimisation is being regularised. An excessive regularisation introduces large systematic errors due to a poor spectral function reconstruction while no regularisation leads to gigantic coefficients. Therefore, it is essential to find the optimal trade-off value for λ.

3.2 HLT method

The HLT method [49] is a modification of the Backus-Gilbert method. In Refs. [50–52] the authors show an important equivalence between this method and the approach based on Gaussian processes. The error functional is indeed the same as $B^{\mathrm{BG}}[\boldsymbol{g}]$, while the $A[\boldsymbol{g}]$ reads

$$A_n^{\mathrm{HLT}}[g_\tau] = \int_{\omega_{\min}}^{\infty} d\omega\, e^{\alpha\omega} \left| \overline{\Delta}_\sigma^{\mathrm{HLT}} - \Delta_\sigma^{\mathrm{HLT}} \right|^2, \tag{11}$$

where the δ-function has been replaced by $\Delta_\sigma^{\mathrm{HLT}}$ and α is a hyper-parameter selecting the type of Jacobi polynomial used in the approximation. In this work we used $\alpha = \{0, 1, -1.99\}$ to select different polynomials and change the speed of convergence of the approximation. The kernel $\Delta_\sigma^{\mathrm{HLT}}$ is a target kernel which is chosen *a priori* to be a smeared version of the δ-function with a smearing radius σ which enters as an input. The minimisation then gives the best approximation of the smearing kernel $\Delta_\sigma^{\mathrm{HLT}}$. Results are obtained using $a_\tau\omega_{\min} \approx 0.05$ and $a_\tau\omega_{\max} = \infty$, however, little to no change is observed changing $\omega_{\min}$.

4. Results

All the linear methods presented above should in principle agree within the given uncertainties, especially for the first peak of the spectral function, corresponding to the ground state. The agreement is found for both low and high temperatures, as shown in Figure 1.

The results corresponding to the Tikhonov method are obtained after applying the Laplace shift technique introduced in Ref. [12]. While the Laplace shift has little to no effect in the Backus-Gilbert and HLT results, it was found empirically to be beneficial for the Tikhonov regularisation. Specifically, the Laplace shift facilitates a faster scan of the hyper-parameter λ. Indeed, one can show that the application of the Laplace shift is equivalent to a change in the coefficients g_τ due to a change in λ.

Information about the ground state mass and decay width of Υ can be extracted by fitting the spectral function to a model Gaussian function. For the Backus-Gilbert and Tikhonov results, the fit is done using all the points leading to the first peak of the spectral function. For the HLT method, we adopt the procedure introduced in Ref. [53], which exploits the fact that we know *a priori* the width of the Gaussian function used to smear the spectral function. This implies that we cannot obtain the decay width from the fit. By checking the quality of the HLT spectral reconstruction we try to use the smallest possible value of σ allowed by the data.

All linear approaches to the inverse problem rely exclusively on the information provided by the given data points. As a result, the quality of the reconstruction progressively deteriorates as the number of time-slices is reduced. In our fixed scale setup, where the temperature of the lattice simulation is increased by reducing the temporal lattice extent, this implies that the

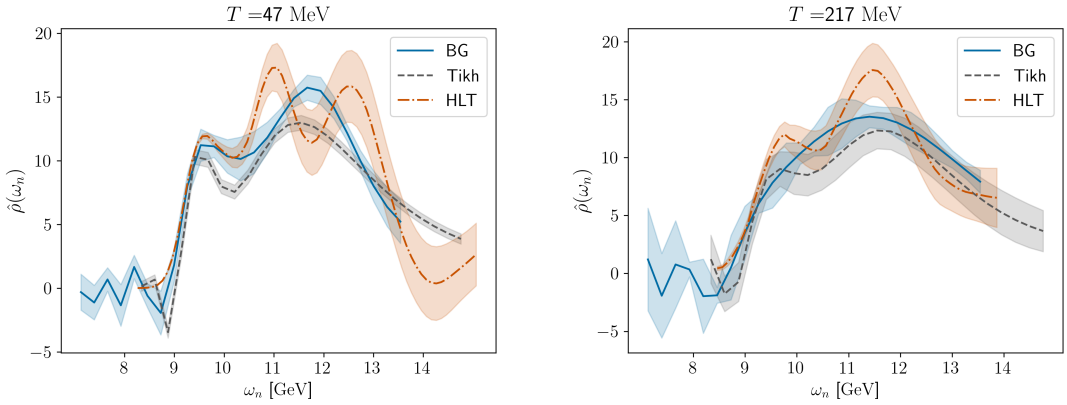

Figure 1: Υ spectral function using the Backus-Gilbert (blue solid line), Tikhonov (dark-gray dashed line) and HLT (dark-orange dashed-dotted line) methods at different values of the temperature.

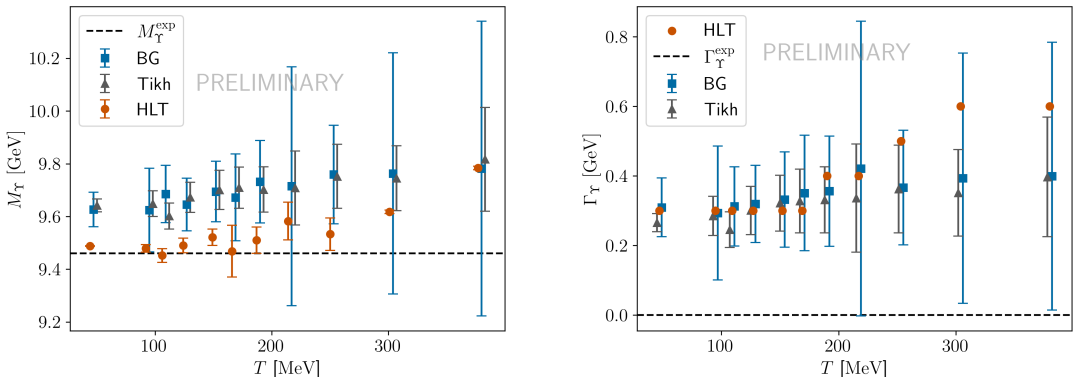

Figure 2: Results of the ground state mass and decay width using the Backus-Gilbert (blue squares), Tikhonov (dark-gray triangles) and HLT (dark-orange circles) methods as a function of temperature. HLT results for the width do not show errorbars since they correspond to input parameters in the minimisation procedure. Results are shifted horizontally to improve readability. The black dashed line correspond to the experimental values at zero temperature.

quality of the spectral function reconstruction progressively worsens with increasing temperature. Unfortunately, this hinders any conclusive statements about the behaviour of spectral functions at high temperatures, which is the region we are most interested in. An imperfect reconstruction inevitably affects the accurate determination of both the position and width of the peaks in the spectral function. Therefore, it is unclear if the broadening of the spectral features is a thermal effect or an artifact of the reconstruction process. In the HLT method, the progressive degradation of the reconstruction forces the use of larger smearing parameter values.

Figure 2 shows the results of the ground state mass and decay width obtained by each method considered in this work. We stress once again that the HLT values of the width are not physical predictions but input parameters.

5. Discussion and Conclusion

The values of the ground state mass show excellent agreement between the Backus-Gilbert and Tikhonov methods and are compatible with the results of the HLT method only for high enough temperatures. At lower temperatures, the HLT method results are more consistent with the experimental value at zero temperature. Overall, the HLT results show a better precision compared to the values obtained with the Backus-Gilbert and Tikhonov methods. This discrepancy can be attributed to the different fitting procedures employed. The lack of a clear peak structure in the spectral function makes the fits of Backus-Gilbert and Tikhonov more susceptible to unwanted excited states which can alter the accurate and precise determination of the ground state peak. This issue is less severe for HLT fits which benefit from the additional information on the smearing width to better constrain the energy states in the spectral function.

The only physical prediction for the decay widths come from the Backus-Gilbert and Tikhonov methods, since, in the HLT method, the width coincides with the smearing width used as input parameter in the regularisation of the inverse problem. Remarkably, the decay widths obtained with all three methods are largely compatible. This suggests that the increase of σ in the HLT method is well justified, considering that the two other methods, which do not rely on fixing the smearing width, obtain similar results.

Unlike the ground state mass, the numerical results for the decay width are significantly larger than the experimental result at zero-temperature, even for the coldest ensemble where thermal effects are negligible. This discrepancy arises due to the finite amount of data available giving a good approximation but never the exact spectral function. The approximation, and consequently the width of the smearing function, depends strongly on the quality of the data. With current state-of-the-art correlators the narrowest smearing function possible has a width corresponding to ≈ 0.3 GeV, which is several orders of magnitude larger than the physical decay width of bottomonium.

The linear methods discussed here provide a completely model-independent approach to the inverse problem. However, they often yield a more conservative estimate of the spectral function compared to non-linear approaches. In other words, spectral functions obtained with non-linear approaches exhibit a clearer and more pronounced peak structure compared to the results of linear methods. Furthermore, the worsening of the spectral reconstruction as we increase the temperature of the system makes the unambiguous identification of thermal effects particularly challenging.

The results of this work will contribute to a comparative study of spectral reconstruction methods to spectral functions at high temperatures, currently being prepared by the FASTSUM collaboration.

Acknowledgments

We are grateful to the HadSpec collaboration for the use of their zero temperature ensembles. A. S. is grateful to Marco Panero, Nazario Tantalo, Alessandro Lupo, Alessandro De Santis, Alessandro Barone and Niccolò Forzano for the numerous stimulating conversations on spectral reconstruction techniques. This work is supported by the UKRI Science and Technology Facilities Council (STFC) Consolidated Grant No. ST/X000648/1.

References

[1] T. Matsui and H. Satz, *J/ψ Suppression by Quark-Gluon Plasma Formation*, *Phys. Lett. B* **178** (1986) 416.

[2] A. Rothkopf, *Heavy Quarkonium in Extreme Conditions*, *Phys. Rept.* **858** (2020) 1 [1912.02253].

[3] CMS collaboration, *Indications of suppression of excited Υ states in PbPb collisions at $\sqrt{S_{NN}} = 2.76$ TeV*, *Phys. Rev. Lett.* **107** (2011) 052302 [1105.4894].

[4] G. Aarts, S. Kim, M.P. Lombardo, M.B. Oktay, S.M. Ryan, D.K. Sinclair et al., *Bottomonium above deconfinement in lattice nonrelativistic QCD*, *Phys. Rev. Lett.* **106** (2011) 061602 [1010.3725].

[5] G. Aarts, C. Allton, S. Kim, M.P. Lombardo, M.B. Oktay, S.M. Ryan et al., *What happens to the Υ and η_b in the quark-gluon plasma? Bottomonium spectral functions from lattice QCD*, *JHEP* **11** (2011) 103 [1109.4496].

[6] G. Aarts, C. Allton, T. Harris, S. Kim, M.P. Lombardo, S.M. Ryan et al., *The bottomonium spectrum at finite temperature from $N_f = 2 + 1$ lattice QCD*, *JHEP* **07** (2014) 097 [1402.6210].

[7] G. Aarts, C. Allton, S. Kim, M.P. Lombardo, S.M. Ryan and J.I. Skullerud, *Melting of P wave bottomonium states in the quark-gluon plasma from lattice NRQCD*, *JHEP* **12** (2013) 064 [1310.5467].

[8] B. Page, C. Allton and S. Kim, *Novel bottomonium results*, *PoS* **LATTICE2022** (2023) 187 [2212.12016].

[9] J.-I. Skullerud et al., *Hadrons at high temperature: An update from the FASTSUM collaboration*, *EPJ Web Conf.* **274** (2022) 05011 [2211.13717].

[10] FASTSUM collaboration, *Recent results from the FASTSUM Collaboration*, *PoS* **LATTICE2022** (2022) 198 [2301.10282].

[11] T. Spriggs et al., *A comparison of spectral reconstruction methods applied to non-zero temperature NRQCD meson correlation functions*, *EPJ Web Conf.* **258** (2022) 05011 [2112.04201].

[12] B. Page, G. Aarts, C. Allton, B. Jäger, S. Kim, M.P. Lombardo et al., *Spectral Reconstruction in NRQCD via the Backus-Gilbert Method*, *PoS* **LATTICE2021** (2022) 134 [2112.02075].

[13] G. Backus and F. Gilbert, *The Resolving Power of Gross Earth Data*, *Geophys. J. Int.* **16** (1968) 169.

[14] F. Gilbert and G. Backus, *Uniqueness in the inversion of inaccurate gross Earth data*, *Phil. Trans. Roy. Soc. A* **266** (1970) 123.

[15] A.N. Tikhonov, *On the Stability of Inverse Problems*, *Proceedings of the USSR Academy of Sciences* **39** (1943) 195.

[16] T. Spriggs et al., *Bottomonium spectral widths at nonzero temperature using maximum likelihood*, *PoS* **LATTICE2021** (2022) 077 [2112.01599].

[17] S. Offler, G. Aarts, C. Allton, B. Jäger, S. Kim, M.-P. Lombardo et al., *Reconstruction of bottomonium spectral functions in thermal QCD using Kernel Ridge Regression*, *PoS* **LATTICE2021** (2022) 509 [2112.02116].

[18] R.G. Edwards, B. Joo and H.-W. Lin, *Tuning for Three-flavors of Anisotropic Clover Fermions with Stout-link Smearing*, *Phys. Rev. D* **78** (2008) 054501 [0803.3960].

[19] D.J. Wilson, R.A. Briceno, J.J. Dudek, R.G. Edwards and C.E. Thomas, *Coupled $\pi\pi$, $K\bar{K}$ scattering in P-wave and the ρ resonance from lattice QCD*, *Phys. Rev. D* **92** (2015) 094502 [1507.02599].

[20] Hadron Spectrum collaboration, *Excited and exotic charmonium spectroscopy from lattice QCD*, *JHEP* **07** (2012) 126 [1204.5425].

[21] Hadron Spectrum collaboration, *Excited and exotic charmonium, D_s and D meson spectra for two light quark masses from lattice QCD*, *JHEP* **12** (2016) 089 [1610.01073].

[22] G. Aarts et al., *Properties of the QCD thermal transition with Nf=2+1 flavors of Wilson quark*, *Phys. Rev. D* **105** (2022) 034504 [2007.04188].

[23] G. Aarts, C. Allton, R. Bignell, T.J. Burns, S.C. García-Mascaraque, S. Hands et al., *Open charm mesons at nonzero temperature: results in the hadronic phase from lattice QCD*, 2209.14681.

[24] G.P. Lepage, L. Magnea, C. Nakhleh, U. Magnea and K. Hornbostel, *Improved nonrelativistic QCD for heavy quark physics*, *Phys. Rev. D* **46** (1992) 4052 [hep-lat/9205007].

[25] D.J. Wilson, R.A. Briceno, J.J. Dudek, R.G. Edwards and C.E. Thomas, *The quark-mass dependence of elastic πK scattering from QCD*, *Phys. Rev. Lett.* **123** (2019) 042002 [1904.03188].

[26] FASTSUM collaboration, *Fastsum generation 2l anisotropic thermal lattice qcd gauge ensembles*, 2024. 10.5281/zenodo.10636046.

[27] W. Jay, *Approaching the Inverse Problem: Toward Lattice QCD Calculations of Inclusive Hadronic Quantities*, *PoS* **LATTICE2024** (2025) 002.

[28] χQCD collaboration, *PDFs and Neutrino-Nucleon Scattering from Hadronic Tensor*, *PoS* **LATTICE2019** (2020) 046 [2008.12389].

[29] J. Bulava, *The spectral reconstruction of inclusive rates*, *PoS* **LATTICE2022** (2023) 231 [2301.04072].

[30] Extended Twisted Mass Collaboration (ETMC) collaboration, *Probing the Energy-Smeared R Ratio Using Lattice QCD*, *Phys. Rev. Lett.* **130** (2023) 241901 [2212.08467].

[31] Extended Twisted Mass collaboration, *Inclusive Hadronic Decay Rate of the τ Lepton from Lattice QCD: The $\bar{u}s$ Flavor Channel and the Cabibbo Angle*, *Phys. Rev. Lett.* **132** (2024) 261901 [2403.05404].

[32] Extended Twisted Mass collaboration, *Inclusive hadronic decay rate of the τ lepton from lattice QCD*, *Phys. Rev. D* **108** (2023) 074513 [2308.03125].

[33] P. Gambino, S. Hashimoto, S. Mächler, M. Panero, F. Sanfilippo, S. Simula et al., *Lattice QCD study of inclusive semileptonic decays of heavy mesons*, *JHEP* **07** (2022) 083 [2203.11762].

[34] R. Kellermann, A. Barone, A. Elgaziari, S. Hashimoto, Z. Hu, A. Jüttner et al., *Systematic effects in the lattice calculation of inclusive semileptonic decays*, *PoS* **LATTICE2024** (2025) 245 [2411.18058].

[35] A. Barone, S. Hashimoto, A. Jüttner, T. Kaneko and R. Kellermann, *Chebyshev and Backus-Gilbert reconstruction for inclusive semileptonic $B_{(s)}$-meson decays from Lattice QCD*, *PoS* **LATTICE2023** (2024) 236 [2312.17401].

[36] R. Kellermann, A. Barone, S. Hashimoto, A. Jüttner*c* and T. Kaneko*a*, *Studies on finite-volume effects in the inclusive semileptonic decays of charmed mesons*, *PoS* **LATTICE2023** (2024) 272 [2312.16442].

[37] A. Barone, S. Hashimoto, A. Jüttner, T. Kaneko and R. Kellermann, *Approaches to inclusive semileptonic $B_{(s)}$-meson decays from Lattice QCD*, *JHEP* **07** (2023) 145 [2305.14092].

[38] P. Gambino and S. Hashimoto, *Inclusive Semileptonic Decays from Lattice QCD*, *Phys. Rev. Lett.* **125** (2020) 032001 [2005.13730].

[39] H. Fukaya, S. Hashimoto, T. Kaneko and H. Ohki, *Towards fully nonperturbative computations of inelastic ℓN scattering cross sections from lattice QCD*, *Phys. Rev. D* **102** (2020) 114516 [2010.01253].

[40] J. Liang, R.S. Sufian, B. Wang, T. Draper, T. Khan, K.-F. Liu et al., *Elastic and resonance structures of the nucleon from hadronic tensor in lattice QCD: implications for neutrino-nucleon scattering and hadron physics*, 2311.04206.

[41] XQCD collaboration, *Towards the nucleon hadronic tensor from lattice QCD*, *Phys. Rev. D* **101** (2020) 114503 [1906.05312].

[42] M. Panero, A. Smecca, N. Tantalo and D. Vadacchino, *The quenched glueball spectrum from smeared spectral densities*, *PoS* **LATTICE2023** (2024) 050 [2311.14806].

[43] N. Forzano et al., *Progress on the spectroscopy of lattice gauge theories using spectral densities*, *PoS* **LATTICE2024** (2025) 137 [2410.11386].

PoS(LATTICE2024)197

[44] E. Bennett et al., *Meson spectroscopy from spectral densities in lattice gauge theories*, *Phys. Rev. D* **110** (2024) 074509 [2405.01388].

[45] M. Bruno, L. Giusti and M. Saccardi, *Spectral densities from Euclidean lattice correlators via the Mellin transform*, 2407.04141.

[46] Y. Burnier, M. Laine and M. Vepsalainen, *Heavy quarkonium in any channel in resummed hot QCD*, *JHEP* **01** (2008) 043 [0711.1743].

[47] M.T. Hansen, H.B. Meyer and D. Robaina, *From deep inelastic scattering to heavy-flavor semileptonic decays: Total rates into multihadron final states from lattice QCD*, *Phys. Rev. D* **96** (2017) 094513 [1704.08993].

[48] G. Bailas, S. Hashimoto and T. Ishikawa, *Reconstruction of smeared spectral function from Euclidean correlation functions*, *PTEP* **2020** (2020) 043B07 [2001.11779].

[49] M. Hansen, A. Lupo and N. Tantalo, *Extraction of spectral densities from lattice correlators*, *Phys. Rev. D* **99** (2019) 094508 [1903.06476].

[50] L. Del Debbio, A. Lupo, M. Panero and N. Tantalo, *Approaches to the Inverse Problem*, in *EuroPLEx Final Conference* [2410.09944].

[51] L. Del Debbio, A. Lupo, M. Panero and N. Tantalo, *Bayesian solution to the inverse problem and its relation to Backus-Gilbert methods*, 2409.04413.

[52] A. Lupo, L. Del Debbio, M. Panero and N. Tantalo, *Bayesian interpretation of Backus-Gilbert methods*, *PoS* **LATTICE2023** (2024) 004 [2311.18125].

[53] L. Del Debbio, A. Lupo, M. Panero and N. Tantalo, *Multi-representation dynamics of SU(4) composite Higgs models: chiral limit and spectral reconstructions*, *Eur. Phys. J. C* **83** (2023) 220 [2211.09581].

PoS(LATTICE2024)197